Journal of
Micro/Nanolithography, MEMS, and MOEMS

Nanolithography.SPIEDigitalLibrary.org

Direct hot embossing of microelements by means of photostructurable polyimide

Meriem Akin
Maher Rezem
Maik Rahlves
Kevin Cromwell
Bernhard Roth
Eduard Reithmeier
Marc Christopher Wurz
Lutz Rissing
Hans Juergen Maier

SPIE.

Meriem Akin, Maher Rezem, Maik Rahlves, Kevin Cromwell, Bernhard Roth, Eduard Reithmeier, Marc Christopher Wurz, Lutz Rissing, Hans Juergen Maier, "Direct hot embossing of microelements by means of photostructurable polyimide," *J. Micro/Nanolith. MEMS MOEMS* **15**(3), 034506 (2016), doi: 10.1117/1.JMM.15.3.034506.

Downloaded From: http://nanolithography.spiedigitallibrary.org/ on 07/21/2017 Terms of Use: http://spiedigitallibrary.org/ss/termsofuse.aspx

Direct hot embossing of microelements by means of photostructurable polyimide

Meriem Akin,[a,*] Maher Rezem,[b] Maik Rahlves,[b] Kevin Cromwell,[a] Bernhard Roth,[b] Eduard Reithmeier,[c] Marc Christopher Wurz,[a] Lutz Rissing,[a] and Hans Juergen Maier[a]
[a]Leibniz Universitaet Hannover, Institute of Micro Production Technology, An der Universitaet 2, 30823 Garbsen, Germany
[b]Leibniz Universitaet Hannover, Hanover Centre of Optical Technologies, Nienburger Straße 17, 30167 Hanover, Germany
[c]Leibniz Universitaet Hannover, Institute of Measurement and Automatic Control, Nienburger Straße 17, 30167 Hanover, Germany

Abstract. While automatic hot embossing systems are available for large- and small-scale productions of polymeric devices, one of the process challenges remains to be the manufacturing of precise, durable, and yet inexpensive hot embossing stamps. The use of metallic stamps manufactured by electroplating a photoresist pattern or by precision milling and their replication into silicone molds with UV-lithography, electroplating, and molding techniques is state of the art. Yet, there have been few, if any, thriving attempts to directly emboss polymers by means of bare photoresists, and in particular polyimide-based photoresists, without transferring the photoresist patterns into a different stamp material. We conduct a proof-of-concept by developing hot embossing stamps based on photosensitive polyimide. We focus primarily on the reliability of the aforementioned stamps throughout the hot embossing cycle and the fidelity of pattern transfer onto polymeric films for different microstructural patterns. © *2016 Society of Photo-Optical Instrumentation Engineers (SPIE)* [DOI: 10.1117/1.JMM.15.3.034506]

Keywords: hot embossing; stamp fabrication; stamp reliability; optical devices; fluidic systems; polyimide.

Paper 16068 received May 9, 2016; accepted for publication Aug. 4, 2016; published online Aug. 23, 2016.

1 Introduction

Hot embossing techniques enable the processing of inexpensive polymers, e.g., as functional materials in optical devices[1] or structural materials in fluidic systems.[2] While automatic hot embossing systems are available for large- and small-scale productions, one of the main challenges remains to be the manufacturing of precise, durable, and yet inexpensive hot embossing stamps. In research and early prototyping, masters made of photoresists[3] patterned by means of photolithography or e-beam lithography are a standard. Due to the limited thermomechanical reliability of conventional photoresists and their poor adhesion to the supporting substrate, generally micromachined silicon wafers,[4] electroplated metallic stamps,[5] and silicone casts[6] of the original photoresist master are conventional work-arounds. On one hand, etched silicon, metallic stamps, or silicone casts counterbalance the high manufacturing costs of the original master by extending lifetime to failure. On the other hand, further processing after photoresist patterning adds to the complexity of the manufacturing process in large-scale productions. There have been few, if any, thriving attempts to directly emboss polymers by means of bare photoresists,[7,8] and in particular polyimide-based photoresists. Here, we completely eliminate the silicone replications, and reinvent the use of photostructurable polyimide for direct hot embossing. Notably, we choose polyimide-based photoresists due to their low surface energy (37 to 44 mJ/m^2),[9,10] which is mainly beneficial for demolding purposes. Therefore, we omit the use of nonstick coatings and any corresponding contamination issues during hot embossing.[11] Moreover, we utilize thermosetting polyimides that exhibit the required mechanical strength and thermal stability at hot embossing temperatures of polymeric materials (150 to 250°C). By means of nanoindentation experiments at room temperature, we have obtained a young's modulus of 4.19 GPa and a surface nanohardness of 415.06 MPa for the polyimide material used in this work that is maintained up to glass transition of the polyimide (300°C). In comparison, SU-8 photoresists that were used for direct hot embossing,[7,8] have a lower glass transition temperature (200°C) and young's modulus (2.0 GPa) as reported by the SU-8 suppliers. Compared to SU-8, polyimide possesses longer polymer chains, which explains its higher thermomechanical stability and compromises, however, the quality of patterning (straightness and smoothness of side walls of patterns) with photolithography. Hence, an appropriate photoinitiator in the chemical composition of the polyimide precursor is necessary to monitor the polyimide pattern geometry. As importantly, we decide on polyimide because of its wide availability and usage in research and industrial settings.

In this work, we conduct a proof-of-concept by developing hot embossing stamps based on photosensitive polyimide ultimately for MEMS and MOEMS applications. We focus primarily on the reliability of the aforementioned stamps throughout the hot embossing cycle and the fidelity of pattern transfer onto polymeric films for different microstructural patterns.

2 Experimental Setup and Methods

We employ a commercially available photosensitive polyimide precursor FUJIFILM Durimide 7320 that we process as described below. Foremost, we avoid any timing lags

*Address all correspondence to: Meriem Akin, E-mail: akin@impt.uni-hannover.de

1932-5150/2016/$25.00 © 2016 SPIE

Downloaded From: http://nanolithography.spiedigitallibrary.org/ on 07/21/2017 Terms of Use: http://spiedigitallibrary.org/ss/termsofuse.aspx

between the processing steps in pursuance of minimizing wrinkling of the functional surface of polyimide, especially with a polyimide thickness of 25 μm and higher. The following process parameters are dependent on the lab conditions and equipment types.

i. *Single layer gyroset spin coating*: In order to guarantee a homogeneous distribution of the embossing pressure, we spin coat the polyimide precursor onto planar and atomically smooth 4 in. to 525-μm thick silicon substrates with an arithmetic surface roughness $R_a < 1.5$ nm, unless otherwise stated. First, we dehydrate the substrates on an open hot plate at 100°C immediately before spin coating to guarantee intact adhesion between polyimide and substrate. Dependent on the heating equipment and process conditions, higher temperatures than 100°C may be necessary to achieve a complete dehydration. Varying the spin coating speed from 10 to 5000 rpm at a spin coating duration of 40 s in a gyroset spin coater Karl Suss RC8, we obtain polyimide layers of thicknesses ranging from 4 to 150 μm in a single spin coating step. In order to achieve a good adhesion between the polyimide and the smooth silicon substrate, we coat the silicon platform with an adhesion promoter that enhances the adhesion of polyimide to silicon or we pattern polyimide onto a silicon wafer precoated with polyimide. The adhesion of the polyimide to the stamp platform is quantified by conducting shear tests on polyimide studs of the anticipated stamp dimensions (polyimide thickness and pattern size). Typically, we obtain a shear strength of 4 to 5.5 $\mathrm{kg/mm^2}$ for both $100 \times 100\ \mu\mathrm{m}^2$ polyimide-on-polyimide and polyimide-on-silicon patterns.

ii. *Soft bake*: Especially required for thicker layers, slow heating at a maximum rate of 5 K/s from room temperature to soft bake temperature, 100°C, is adopted. It is to be noted that the duration of soft bake increases with increasing thickness of the polyimide layer. For reference purposes, soft bake times of final coating thicknesses below 25 μm should not exceed 10 min. In addition, in order to reduce coating stresses in thick polyimide coatings, a presoft bake at 70°C is necessary before increasing the soft bake temperature to 100°C. Finally, unprompted cooling down to room temperature is necessary for further processing.

iii. *Contact illumination*: Employing the contact aligner Karl Suss MA6 and a chrome-on-glass photomask (Delta Mask b.v.), we illuminate the polyimide coatings with conventional UV (350 to 450 nm) radiation at peak wavelengths 365, 405 and 438 nm with the intensities 100%, 70%, and 55%, respectively. Here, an illumination power of 13.6 $\mathrm{mW/cm^2}$ is adopted, whereas the duration of illumination and post exposure crosslinking depend on the thickness of the coating. For instance, a 13-μm thick coating is illuminated for 30 s at the aforementioned illumination power, whereas a postexposure crosslinking of 30 min is sought to be sufficient. With the increase in the soft bake time past evaporation of the solvent content, the illumination duration is expected to increase as well. Using an i-line filter, a sharper patterning of the polyimide may be achieved. Some commercial polyimides come with photoinitiators that are sensitive to 350 nm only, and the use of an i-line filter is not necessary.

iv. *Immersion development*: In order to ensure impeccable development of the polyimide patterns, any prior contact of the illuminated polyimide with nitrogen past the regular nitrogen content in the air, e.g., through blow drying with a nitrogen gun or the like, and with solvents should be avoided. Employing the polyimide developers QZ3501 and QZ3512, we immerse the illuminated polyimide samples in development baths in the following order: (1) QZ3501, (2) (50%-QZ3501, 50%-QZ3512), (3) QZ3512, (4) QZ3501 for a few seconds in each bath until wetting of the functional surface occurs, and repeat iteratively until optical inspection confirms complete development. With the increase in coating thickness and illumination time, immersion development takes longer. Finally, development remnants are rinsed using isopropyl alcohol and blow dried by means of nitrogen. Particularly, a successful development is obtained once a decrease in thickness does not exceed 5% of the predevelopment thickness, and discoloring of the QZ3512-bath does not occur.

v. *Imidization*: Under nitrogen flow, the developed polyimide samples are heated at a rate of 5 K/s from room temperature to 350°C, which is held for 60 min consecutively. Subsequently, the samples are cooled down to room temperature while maintaining nitrogen flow. Upon successful imidization, the polyimide layers shrink mainly in thickness by 30% to 50%.

vi. In a mass production setting, multiple stamps could be prepared in parallel to compensate for the process layovers. Since immersion development is a time-intensive technique to develop polyimides, atomized spray development should be employed in a mass production setting. Adopting atomized spray development, a development process including rinsing and drying for a coating thickness of 25 μm takes below 1 min.

Thereafter, we employ the polyimide stamps for hot embossing of micropatterns onto 1-mm thick poly(methyl methacrylate) films in analogy to the process as described in Ref. 12. In particular, we emboss periodic rib and trench (positive and negative) patterns in the range of [5,80] μm in thickness and [50,200] μm in width. Accordingly, the hot embossing stamp-hot embossed polymer mates are brought into intimate contact in the nanoimprinter Jenoptik Hex03. Notably, the hot embossing cycle except for demolding and wedge correction is automated. Knowing that the glass transition temperature of the poly(methyl methacrylate) film, an off-the-shelf product, lies in average at 105°C, we have opted for 140°C as a hot embossing temperature, where we observe the poly(methyl methacrylate) film to successfully flow and inherit the stamp pattern, largely for all batches, as investigated in Ref. 12. Subject to vacuum conditions, top and bottom heating at 140°C, and an embossing pressure of 0.76 MPa, a duration of 180 s is determined to sufficiently allow for filling of the stamp cavities by action of polymer flow. When stamp and polymer are cooled down to 40°C, demolding is conducted manually. Embossing stamps (ST) and embossed poly(methyl methacrylate) films (PM) are inspected by means of confocal laser scanning microscopy Keyence VK-9710, whereas a laser wavelength of 408 nm is utilized. Positioning of the measurement locations under the laser scanning microscope was done manually

Downloaded From: http://nanolithography.spiedigitallibrary.org/ on 07/21/2017 Terms of Use: http://spiedigitallibrary.org/ss/termsofuse.aspx

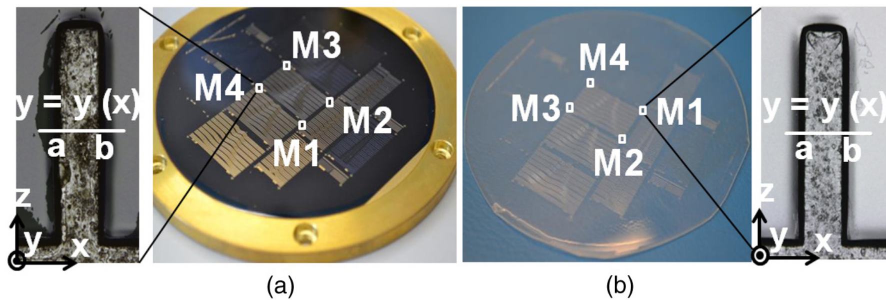

Fig. 1 Measurement locations (M1, M2, M3, and M4) on (a) a-4 in. embossing stamp (ST) and (b) a-4 in. embossed poly(methyl methacrylate) film (PM) and micrographs of the corresponding measured patterns. The illustrated horizontal line $y = y(x)$ over the range $x = [a, b]$ denotes the location of the extracted 2-D profile from the scanned pattern.

without the use of precision positioning. Despite extreme care, the pattern lateral location was not positioned in the exact same way with respect to the microscope imaging frame, which causes a slight visualization shift in the width direction. Unless otherwise stated, four locations (M1, M2, M3, M4) per region of interest are scanned from which a two-dimensional (2-D) profile per region is extracted. The 2-D profiles were extracted manually from the scanned patterns, and hence, do not lie for two different measurements at the exact same location on the scanned region. Knowing that the spin-coating process induces a nonplanarity, i.e., slight variations in thickness, to the free surface of the polyimide coating despite the planarity of the stamp platform, the variation in thickness for the same pattern and platform is reflected in the extraction method of the 2-D profiles. In particular, we extract 2-D profiles of the measured locations (Fig. 1) and scrutinize their geometrical attributes.

Figure 2 exemplarily shows scanning electron micrographs of embossed patterns.

3 Results and Discussion

3.1 *Replication of Trench Patterns of [5,80] μm in Thickness*

In this section, we investigate the fidelity of pattern transfer from a polyimide micropattern of varying thickness (5, 29, and 80 μm) obtained by hot embossing. In particular, we employ trench patterns at the stamp level that are 100-μm wide. We inspect the surface profile of the stamp patterns before and after hot embossing, and compare them with the resulting hot embossed patterns (Fig. 3, Table 1). While polyimide patterns that are <30 μm in thickness delivered impeccable results within the limitations of the measurement method, hot embossing by means of 80-μm thick polyimide patterns failed, mainly due to the original quality of the polyimide pattern. In particular, a deficit in the definition of the side walls of the 80-μm patterns was observed after polyimide development and is to be related to the limitations of thick single-layer spin coating of the polyimide precursor. In addition, the existing undulations in the polyimide side walls were deformed due to demolding and are expected to affect the reproducibility of the pattern transfer throughout subsequent hot embossing cycles.

3.2 *Replication of Trench and Rib Micropatterns*

Hot embossing with trench patterned stamps is traditionally known to be less delicate than hot embossing with rib patterned stamps.[13] In this work, while the patterns are shaped by polyimide, mechanical support of the patterns is granted by common surface areas of the polyimide and the silicon substrate. In the case of a trench-shaped pattern, the surface area, and hence, the mechanical support to the pattern, are larger than those of a rib-shaped pattern. Hence, for the same embossing load, the rib patterns are subject to a higher hot embossing and demolding pressure, which may exceed their deformation yielding point. Consequently, the fidelity of replication of trench patterned stamps is expected to be superior.

In order to investigate the aforementioned hypothesis, we hot emboss trench and rib patterns of a thickness of 5 μm (Fig. 4), since the stability of replication of the trench counterpart was confirmed in Sec. 3.1. In addition, we focus on the pattern transfer of micropatterns of 50, 100, and 200 μm in width. In this investigation, we measure only two locations per region of interest, as observed in the forthcoming to be sufficient for a consistent analysis.

Certainly, the deviation between the geometry of the hot embossing stamp—before and after hot embossing—and the hot embossed polymer is negligible for the trench patterns when compared to the rib counterparts (Figs. 5 and 6). As shown in Table 2, the range of deviation in width and height of the rib-shaped patterns is larger than for the trench-shaped patterns, which confirms the instability of the polyimide ribs for hot embossing. In addition to the nonfidelity of replication, the distortion of the rib patterns according to the Poisson effect is of fundamental consequence on the reliability of the hot embossing process. Finally, the convex front shape of the rib patterns due to shrinking in the imidization process as depicted in Fig. 4(b) is noted and needs to be considered if crucial to a specific application. For instance, the convex shape may serve as an optical element, such as a lens, if embedded in an optical device.

3.3 *Reliability Testing of Embossing Stamps*

In this study, we focus the attention on the thermomechanical reliability of polyimide for hot embossing purposes. For this reason, we avoid the failure of other stamp constituents prior to the failure of polyimide. Hence, we eliminate the silicon substrate due to its brittleness and prior failure to the polyimide in the presence of wedge errors between stamp and polymeric film. Instead, we employ a 5-mm thick brass plate with a surface roughness given by the arithmetic average $R_a = 0.215$ μm as a substrate for polyimide. Even

Downloaded From: http://nanolithography.spiedigitallibrary.org/ on 07/21/2017 Terms of Use: http://spiedigitallibrary.org/ss/termsofuse.aspx

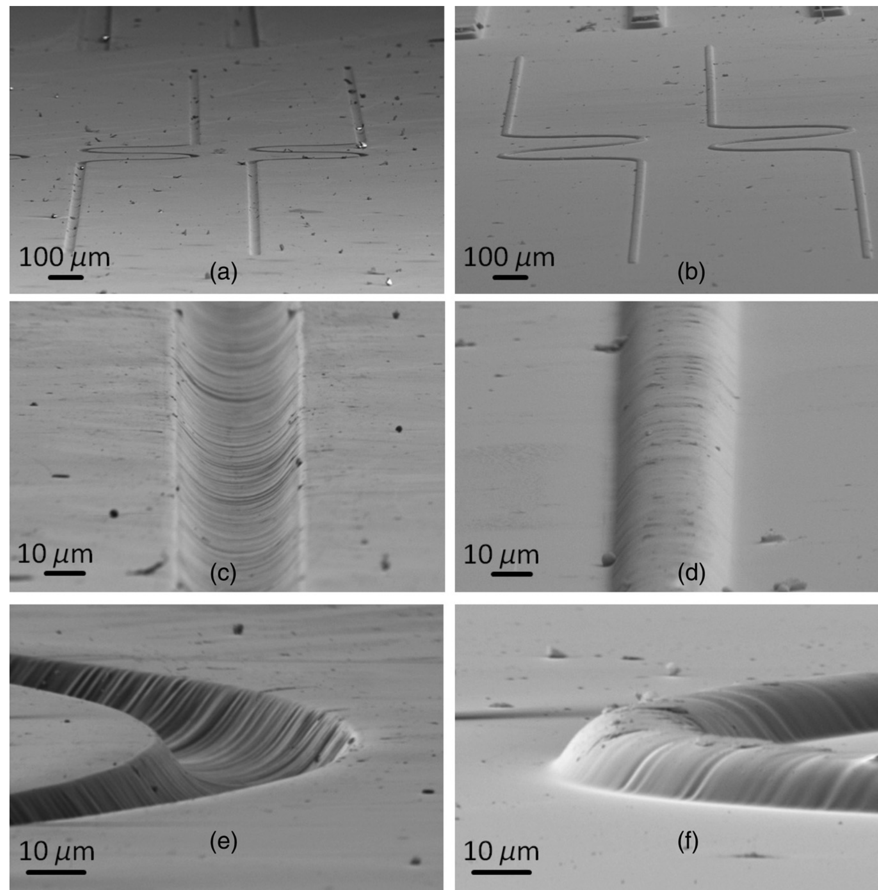

Fig. 2 Scanning electron micrographs of exemplary embossed trench patterns from (a), (c), and (e) polyimide stamp onto (b), (d), and (f) polymeric film.

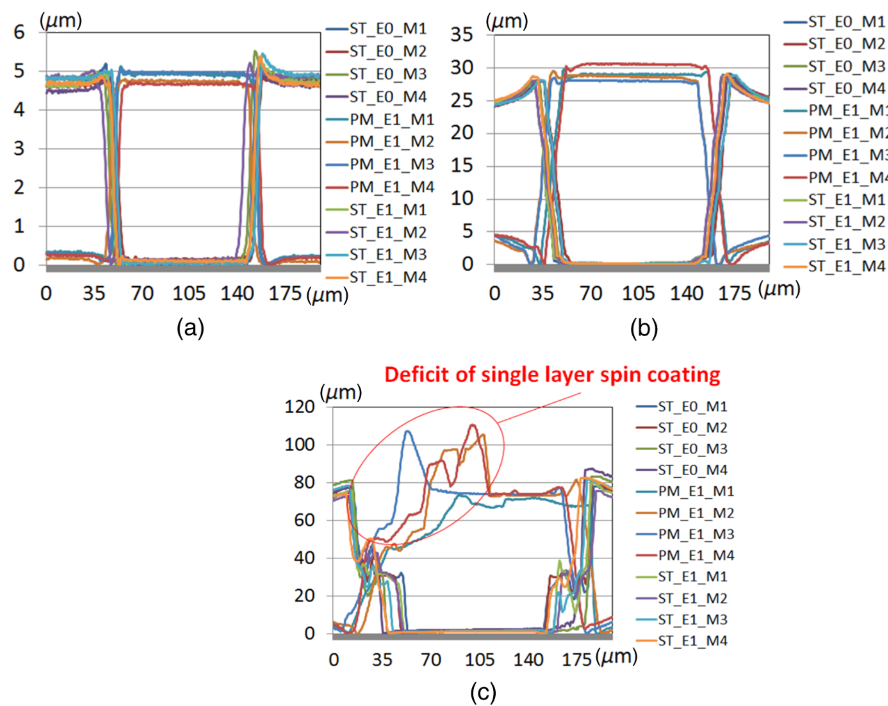

Fig. 3 Pattern transfer from a polyimide micropattern of (a) 5-μm, (b) 29-μm, and (c) 80-μm thickness onto polymer film and comparison of stamp condition before and after hot embossing.

Downloaded From: http://nanolithography.spiedigitallibrary.org/ on 07/21/2017 Terms of Use: http://spiedigitallibrary.org/ss/termsofuse.aspx

Table 1 Replication of 100-μm wide trench patterns of $[5, 80]$ μm in thickness: average deviations in pattern width and height due to the hot embossing process. δ_w^{ST} and δ_h^{ST} are the deviations in pattern width and height, respectively, on a stamp after one hot embossing cycle. $\delta_w^{ST\text{-}PM}$ and $\delta_h^{ST\text{-}PM}$ are the deviations in pattern width and height, respectively, between stamp and embossed polymer.

Anticipated height (μm)	$\vert\delta_w^{ST}\vert$ (%)	$\vert\delta_h^{ST}\vert$ (%)	$\vert\delta_w^{ST\text{-}PM}\vert$ (%)	$\vert\delta_h^{ST\text{-}PM}\vert$ (%)
5	1.144	4.43	2.59	3.88
29	0.31	0.58	1.86	2.14
80	0.49	2.7	0.15	20.73

though not originally anticipated, the surface roughness of the brass plate is expected to enhance the adhesion of polyimide to the supporting substrate by means of mechanical interlocking, and is sought to be beneficial for the stamp reliability. Yet, the surface roughness induces nonplanarity of the coating in addition to the nonplanarity due to the spin coating process, which needs to be considered carefully for applications with rigorous requirements on surface smoothness. Compared to the silicon wafer used previously, the brass plate is not as highly planarized.

In order to evaluate the long-term reliability of the stamp, we track the evolution of the shape of a micropattern (100-μm wide and 29-μm thick as prescribed by the lithography mask and the spin coating process) over

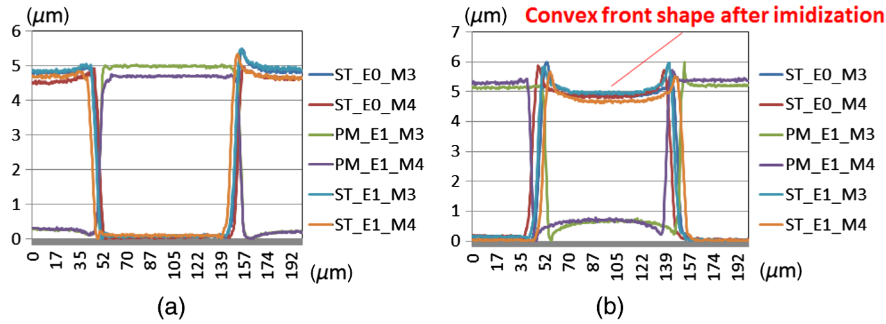

Fig. 4 Exemplary surface profiles of the replication of (a) trench and (b) rib patterns.

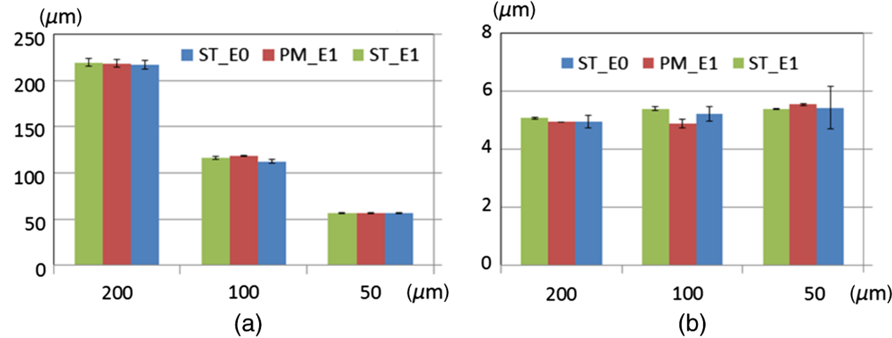

Fig. 5 (a) Width and (b) thickness of stamp (before and after embossing) and hot embossed polymer of a trench pattern for micropatterns of 50, 100, and 200 μm in width.

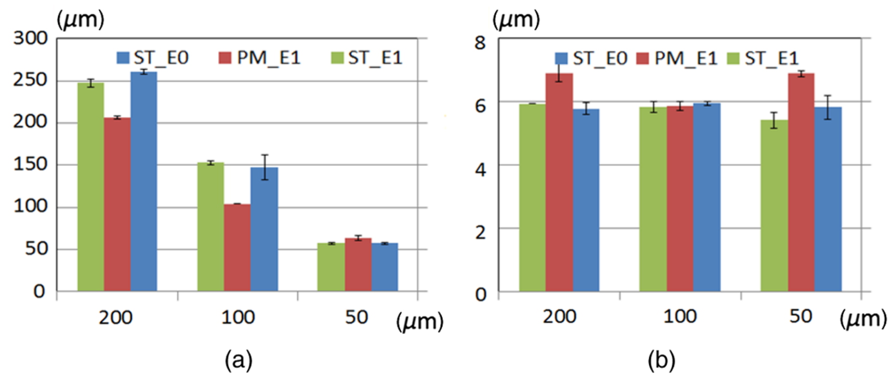

Fig. 6 (a) Width and (b) thickness of stamp and hot embossed polymer of a rib pattern for micropatterns of 50, 100, and 200 μm in width.

Downloaded From: http://nanolithography.spiedigitallibrary.org/ on 07/21/2017 Terms of Use: http://spiedigitallibrary.org/ss/termsofuse.aspx

Table 2 Replication of trench and rib micropatterns: average deviations in width and thickness due to the embossing process. δ_w^{ST} and δ_h^{ST} are the deviations in pattern width and height, respectively, on a stamp after one hot embossing cycle. $\delta_w^{ST\text{-}PM}$ and $\delta_h^{ST\text{-}PM}$ are the deviations in pattern width and height, respectively, between stamp and embossed polymer.

Anticipated width	$\lvert\delta_w^{ST}\rvert$ (%)	$\lvert\delta_h^{ST}\rvert$ (%)	$\lvert\delta_w^{ST\text{-}PM}\rvert$ (%)	$\lvert\delta_h^{ST\text{-}PM}\rvert$ (%)
50 μm—trench	0.12	0.73	0.53	2.11
100 μm—trench	3.41	3.55	5.27	6.41
200 μm—trench	1.04	2.64	0.48	0.17
50 μm—rib	0.12	7.01	11.61	18.37
100 μm—rib	3.53	1.88	29.36	1.31
200 μm—rib	5.08	2.69	20.72	19.44

50 hot embossing cycles in a nonaccelerated manner (Figs. 7 and 8).

Up to the 50th cycle, no major deterioration of the hot embossing stamp was observed except at location M2, where polyimide started to peel off, mainly due to demolding artifacts,[14] and due to nonreproducibility in manual demolding. When approaching the 50th embossing cycle, the variation in the stamp dimensions is due to the failure mode seen while demolding. All other variations prior to failure are due to the limitations in the measurement method and the spin coating process in combination with the nonplanarity and roughness of the underlying brass platform that induce a variation in coating thickness across the stamp. Clearly, the deviation range should match the requirements of the anticipated device and could be compensated by using a highly planar and smooth stamp platform. As significant is the observed recurrence of frictionless demolding of the polymer film from the hot embossing stamp in the absence of any surface pretreatment and nonstick coatings. In

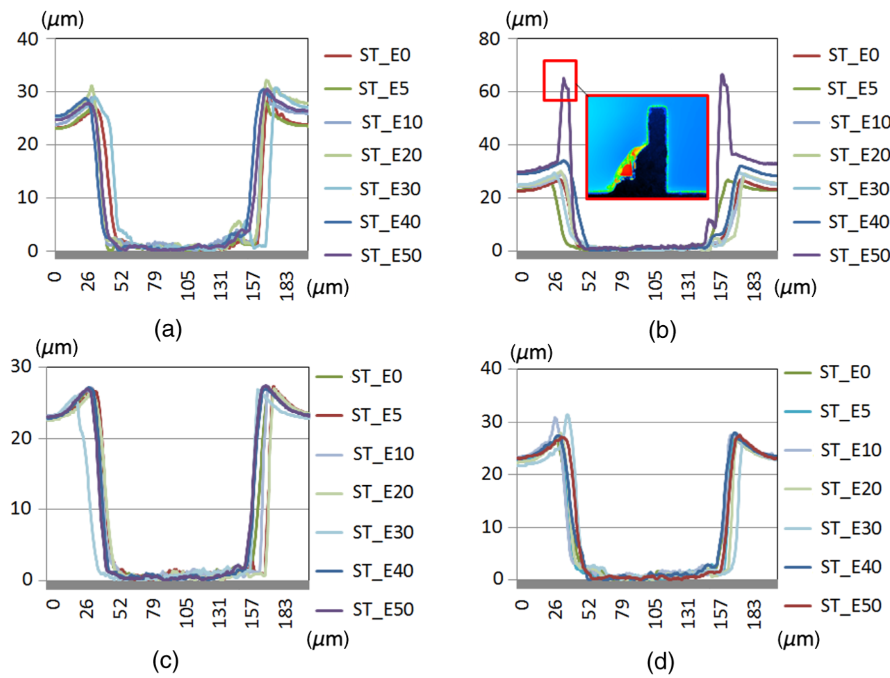

Fig. 7 Profile of 50-μm wide 25-μm thick trench patterns at four locations [(a) M1, (b) M2, (c) M3, and (d) M4] of the embossing stamp (ST) for 50 consecutive embossing cycles.

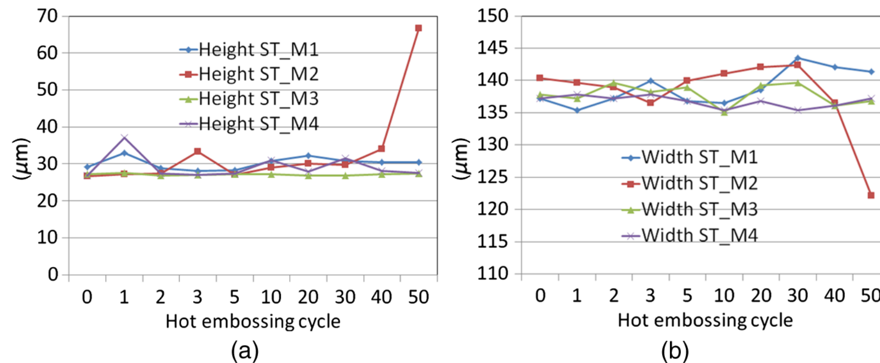

Fig. 8 Evolution of (a) height and (b) width of stamp micropatterns at four measurement locations (M1, M2, M3, M4) more than 50 embossing cycles.

Downloaded From: http://nanolithography.spiedigitallibrary.org/ on 07/21/2017 Terms of Use: http://spiedigitallibrary.org/ss/termsofuse.aspx

addition, optical inspection confirmed the nonexistence of any contaminants on the hot embossed polymer film.

4 Summary and Outlook

In this paper, we have demonstrated the use of polyimide as a stamp material for direct hot embossing of micropatterns onto thermoplastics. We argue that this approach of stamp fabrication is profitable for spatially sparse and dense devices (MEMS and MOEMS) that can be manufactured in a roll-to-roll approach. First, we have verified the reliability of the polyimide stamps and frictionless demolding in the absence of any surface pretreatment and nonstick coatings up to 50 hot embossing cycles. In addition, we have demonstrated impeccable replication of trench patterns in the width range [50,200] μm within the limitations of single layer spin coating of the polyimide precursor. Moreover, we have expounded the inferior embossing quality of rib patterns, which can be optimized when demolding is adjusted and automated. Also, by automating demolding, the long-term reliability of the polyimide stamp is expected to increase. In order to deliver thick patterns (80 μm and above) and well-defined geometries of the polyimide stamps, we propose multilayer spin coating and postexposure bake to counteract undulation of the polyimide side walls. As for optical applications, the surface roughness of the polyimide patterns needs to be monitored rigorously, which is the focus of a follow-up work.

Appendix

Let a 2-D surface profile of a micropattern extracted from the confocal laser scanning microscope measurements be described as $y = y(x)$, whereas $x \in [a, b]$. The height h of the profile is calculated as follows: $h = \max_{x\in[a,b]} y(x) - \min_{\in[a,b]} y(x)$. For a trench pattern, the width w of the stamp profile (ST) and the corresponding embossed profile (PM) are given by

$$w_{\mathrm{ST}}^{t} = y^{-1}\left[\max_{x\in\left[\frac{a+b}{2},b\right]} y(x)\right] - y^{-1}\left[\max_{x\in\left[a,\frac{a+b}{2}\right]} y(x)\right],$$

$$w_{\mathrm{PM}}^{t} = y^{-1}\left[\min_{x\in\left[\frac{a+b}{2},b\right]} y(x)\right] - y^{-1}\left[\min_{x\in\left[a,\frac{a+b}{2}\right]} y(x)\right],$$

respectively, whereas for a rib pattern, the width of the stamp profile and the corresponding embossed profile are given by

$$w_{\mathrm{ST}}^{r} = y^{-1}\left[\min_{x\in\left[\frac{a+b}{2},b\right]} y(x)\right] - y^{-1}\left[\min_{x\in\left[a,\frac{a+b}{2}\right]} y(x)\right],$$

$$w_{\mathrm{PM}}^{r} = y^{-1}\left[\max_{x\in\left[\frac{a+b}{2},b\right]} y(x)\right] - y^{-1}\left[\max_{x\in\left[a,\frac{a+b}{2}\right]} y(x)\right].$$

In the remaining, we denote by En the embossing cycle, where $n \in \mathbb{N}$. In addition, the expressions $\mathrm{ST}En$ and $\mathrm{PM}En$ prescribe the status of stamp and embossed polymer after n embossing cycles, where $n \in \mathbb{N}$. Finally, $\mathrm{ST}EnMm$ and $\mathrm{PM}EnMm$ designate the status of stamp and embossed polymer after n embossing cycles at location Mm, where $n \in \mathbb{N}$ and $m \in \{1,2,3,4\}$, respectively. Consequently, the average deviations in pattern width and height due to the embossing process are calculated. The average deviation in stamp width before and after embossing in percent is given by

$$\delta_w^{\mathrm{ST}} = \frac{1}{4}\sum_m \frac{w_{\mathrm{ST}E1Mm} - w_{\mathrm{ST}E0Mm}}{w_{\mathrm{ST}E0Mm}} \times 100.$$

The average deviation in stamp thickness before and after embossing in percent is

$$\delta_h^{\mathrm{ST}} = \frac{1}{4}\sum_m \frac{h_{\mathrm{ST}E1Mm} - h_{\mathrm{ST}E0Mm}}{h_{\mathrm{ST}E0Mm}} \times 100.$$

The average deviation in pattern width in percent between stamp and polymer film reads

$$\delta_w^{\mathrm{ST\text{-}PM}} = \frac{1}{4}\sum_m \frac{w_{\mathrm{ST}E0Mm} - w_{\mathrm{PM}Mm}}{w_{\mathrm{ST}E0Mm}} \times 100.$$

Finally, the average deviation in pattern height between stamp and polymer film is

$$\delta_h^{\mathrm{ST\text{-}PM}} = \frac{1}{4}\sum_m \frac{h_{\mathrm{ST}E0Mm} - h_{\mathrm{PM}Mm}}{h_{\mathrm{ST}E0Mm}} \times 100.$$

Acknowledgments

This work was supported by the German Research Foundation under the collaborative research center "Planar Optronic Systems." We acknowledge F. Barnikol, E. De Meersman, and A. Lubbers from Fujifilm Electronic Materials for their technical support with the development of the hot embossing stamps. We also acknowledge M. Stompe for conducting the nanoindentation measurements on polyimide and F. Dencker for taking the SEM micrographs of the stamps.

References

1. C.-G. Choi et al., "Fabrication of large-core 1 × 16 optical power splitters in polymers using hot-embossing process," *IEEE Photonics Technol. Lett.* **15**(6), 825–827 (2003).
2. J. L. Charest et al., "Hot embossing for micropatterned cell substrates," *Biomaterials* **25**(19), 4767–4775 (2004).
3. M. B. Esch et al., "Influence of master fabrication techniques on the characteristics of embossed microfluidic channels," *Lab Chip* **3**, 121–127 (2003).
4. H. Becker and U. Heim, "Silicon as tool material for polymer hot embossing," in *Twelfth IEEE Int. Conf. on Micro Electro Mechanical Systems*, pp. 228–231 (1999).
5. L. J. Heyderman et al., "Nanofabrication using hot embossing lithography and electroforming," *Microelectron. Eng.* **57–58**, 375–380 (2000).
6. J. Narasimhan and I. Papautsky, "Polymer embossing tools for rapid prototyping of plastic microfluidic devices," *J. Micromech. Microeng.* **14**, 96–103 (2003).
7. J. Zhang et al., "Polymerization optimization of SU-8 photoresist and its applications in microfluidic systems and MEMS," *J. Micromech. Microeng.* **11**(20), 20–26 (2001).
8. K. Huikko et al., "Poly(dimethylsiloxane) electrospray devices fabricated with diamond-like carbonpoly(dimethylsiloxane) coated SU-8 masters," *Lab Chip* **3**, 67–72 (2003).
9. K. Gotoh, *Polymer Surface Modification: Relevance to Adhesion*, Vol. **3**, pp. 129–132, Vision Sports Publishing, Leiden, Boston (2004).
10. N. Inagaki, S. Tasaka, and K. Hibi, *Plasma Surface Modification of Polymers: Relevance to Adhesion*, p. 280, Vision Sports Publishing, Zeist, The Netherlands (1994).
11. R. W. Jaszweski et al., "The deposition of anti-adhesive ultra-thin Teflon-like films and their interaction with polymers during hot embossing," *Appl. Surf. Sci.* **143**(1–4), 301–308 (1999).
12. M. Rezem et al., "Hot embossing of polymer optical waveguides for sensing applications," in *Procedia Technology, 2nd Int. Conf. on System-Integrated Intelligence: Challenges for Product and Production Engineering*, Vol. 15, pp. 514–521 (2014).
13. H. S. Nalwa, *Handbook of Thin Film Materials, Technology and Engineering*, Vol. **5**, p. 24, Academic Press, San Diego, California (2001).

Downloaded From: http://nanolithography.spiedigitallibrary.org/ on 07/21/2017 Terms of Use: http://spiedigitallibrary.org/ss/termsofuse.aspx

14. M. Dirckx, H. K. Taylor, and D. E. Hardt, "High-temperature de-molding for cycle time reduction in hot embossing," in *Proc. Society of Plastics Engineers Annual Technical Conf.*, pp. 2972–2976 (2007).

Meriem Akin received her bachelor's and master's degrees in computational engineering from the Leibniz University of Hanover, Hanover, Germany, in 2006 and 2008, respectively, and her master's degree in mechanical engineering and electrical engineering and computer sciences from the University of California at Berkeley, Berkeley, California, USA, in 2011 and 2014, respectively. She is currently a research associate with the Institute of Micro Production Technology, Leibniz University of Hanover. Her current research interests include the reinvention of the material paper as an engineering material for developing equitable technology.

Maher Rezem received his diploma degree in electrical engineering in 2012 from the Karlsruhe Institute of Technology. He is currently pursuing his PhD in engineering at the Hanover Center for Optical Technologies (HOT) of the Leibniz University Hanover. He is working in the field of polymer optics manufacturing by means of hot embossing and UV-imprinting.

Maik Rahlves received his diploma degree in physics in 2006 and his PhD in mechanical engineering in 2011 from the Carl-von-Ossietzky University and Leibniz University Hanover, respectively. Since 2009, he has been with the Hanover Center for Optical Technologies, Leibniz University Hanover, where he has headed the applied optics group since 2011. His research interests are optical metrology, holography, and polymer-based micro-optics.

Kevin Cromwell is a master's student in nanotechnology with designated emphasis in mechanical engineering and optics at Leibniz University of Hanover. Since 2013, he has been a student assistant at the Institute of Micro Production Technology working on the development of hot embossing stamps, metallization processes, and eutectic bonding techniques.

Bernhard Roth received his PhD from the University Bielefeld in atomic physics in 2001. From 2002 to 2007, he was a group leader at the University Duesseldorf, where he obtained his state doctorate (Habilitation) in quantum optics. Since 2012, he has been director of the Hanover Center for Optical Technologies (HOT) and professor of physics at the Leibniz University Hanover. His activities include laser development and spectroscopy, polymer optical sensing, as well as biomedical optics and imaging.

Eduard Reithmeier received his diploma degree in mechanical engineering in 1977 and mathematics in 1979 from the Technical University Munich. In 1989, he also obtained his PhD in mechanical engineering from the same university. From 1992 to 1996, he was technical director (automation and medical engineering) at Bodenseewerk Geraetetechnik GmbH. Since 1996, he has been a professor of mechanical engineering at the Institute for Measurement and Control, Leibniz University Hanover. His activities include optical imaging, acoustics, production measurement, and control theory.

Marc Christopher Wurz received his diploma degree in civil engineering and his PhD in mechanical engineering from the Leibniz Universitaet Hannover. He is a senior engineer of the Institute of Micro Production Technology (IMPT) of the Leibniz University Hanover.

Lutz Rissing received his Doctor of Engineering degree in mechanical engineering from the University of Hanover, Hanover, Germany, in 1999. He has been a professor and the chair of the Institute of Micro Production Technology with the Department of Mechanical Engineering, Leibniz University of Hanover, Hanover, Germany, since 2010. He has authored and coauthored more than 100 conference papers, journal papers, and book chapters. His current research interests include design and fabrication of precise MEMS mainly based on magnetic effects.

Hans Juergen Maier received his doctoral degree in materials science from the University of Erlangen-Nurnberg. He is a professor at the Faculty of Mechanical Engineering of the Leibniz Universitaet Hannover, director of the Institut fur Werkstoffkunde (materials science), and spokesman of DFG's research unit on high-temperature shape memory materials.

Downloaded From: http://nanolithography.spiedigitallibrary.org/ on 07/21/2017 Terms of Use: http://spiedigitallibrary.org/ss/termsofuse.aspx